54th AIAA Aerospace Sciences Meeting
4 - 8 Jan 2016, San Diego, CA
AIAA-2016-1459

Studies of Flow Topology around Hemisphere at Transonic Speeds Using Time-Resolved Oil Flow Visualization

Stanislav Gordeyev[1], Alexander Vorobiev [2], Eric Jumper[3]
University of Notre Dame, Notre Dame, Indiana, 46545

Sivaram Gogineni[4]
Spectral Energies, LLC, Dayton, OH 45431

and

Donald J. Wittich[5]
Air Force Research Laboratory, Directed Energy Directorate, Kirtland AFB, NM 87117

This paper presents the results of the study of surface flow topology over a hemisphere using time-resolved oil flow visualization at a range of Mach numbers between 0.2 and 0.7. Several cameras were used to simultaneously record temporal evolution of oil luminescence on and around the hemisphere. Perspective Transformation Matrix technique was used to reconstruct the spatial distribution of oil luminescence over the "virtual" surface; this approach allows studying oil flow visualization patterns from angles, not directly accessible in the experiment. The separation region downstream of the hemisphere was found to continuously decrease with the increasing Mach number and a formation of a large vortical structure at the separation line near the bottom of the hemisphere was observed at M = 0.7.

I. Introduction

A side-mounted turret is a convenient configuration to use for pointing-and-steering a laser beam from an airborne platform. In the last few years due to an increased interest to use turrets at high transonic and supersonic speeds, research of the flow features around side-mounted turrets and the related aero-optical effects [1] at these speeds has intensified. For flight speeds faster than M = 0.55, a local supersonic region with an ending unsteady shock appears on the turret [2,3]. Recent flight data [4] from AAOL-T [5] and tunnel tests [6,7] at a range of subsonic and transonic speeds have showed that the unsteady shock leads to increased aero-optical distortions, when the laser beam passes directly through the shock. In addition, the shock affects the separated region downstream of the turret due to the shock-wake interaction [6,7,8].

To better understand the effect of the unsteady shock on the flow around the turret, aerodynamic data should be collected along with the aero-optical data. Simultaneous surface-pressure and aero-optical distortions on a cylindrical turret [8] and a hemisphere [7] revealed the presence of the lock-in dynamical mechanism between the shock and the separated wake. Several numerical simulations [9,10] of the flow around a hemisphere at different subsonic, transonic and supersonic speeds showed the changes in the flow features around the hemisphere

[1] Research Associate Professor, Department of Mechanical and Aerospace Engineering, Hessert Laboratory for Aerospace Research, Notre Dame, IN 46556, AIAA Associate Fellow.
[2]Post-Doctoral Assistant, Department of Mechanical and Aerospace Engineering, Hessert Laboratory for Aerospace Research, Notre Dame, IN 46556, AIAA Member.
[3]Professor, Department of Mechanical and Aerospace Engineering, Hessert Laboratory for Aerospace Research, Notre Dame, IN 46556, AIAA Fellow.
[4]President, 5100 Springfield St. Suite 301, Dayton OH 45431, Senior AIAA Member.
[5]Aerospace Engineer, Laser Division, 3550 Aberdeen Ave SE.

due to the presence of the shock. This paper experimentally studies the changes of the surface flow topology on and around the hemisphere using a time-resolved oil visualization technique.

II. Experimental Set-Up

Measurements of the surface flow topology around a 10-inch hemisphere at different transonic Mach numbers of 0.2, 0.5, 0.6 and 0.7 were performed in White Field tunnel using time-resolved oil-visualization technique. The range of Reynolds numbers based on the incoming speed and the hemisphere diameter were in the range of 1 million for M = 0.2 up to 2.9 million for M = 0.7. The test section size is 3 ft x 3ft x 9 ft. Thick mineral oil with a small addition of UV-dye was applied to the full surface of the hemisphere, as well as the tunnel wall around it. The UV-light sources were placed on both sides of the tunnel to visualize the oil, see Figure 1, as the dye fluoresces in UV-light and the intensity of the emitted light can be assumed to be proportional to the local oil thickness.

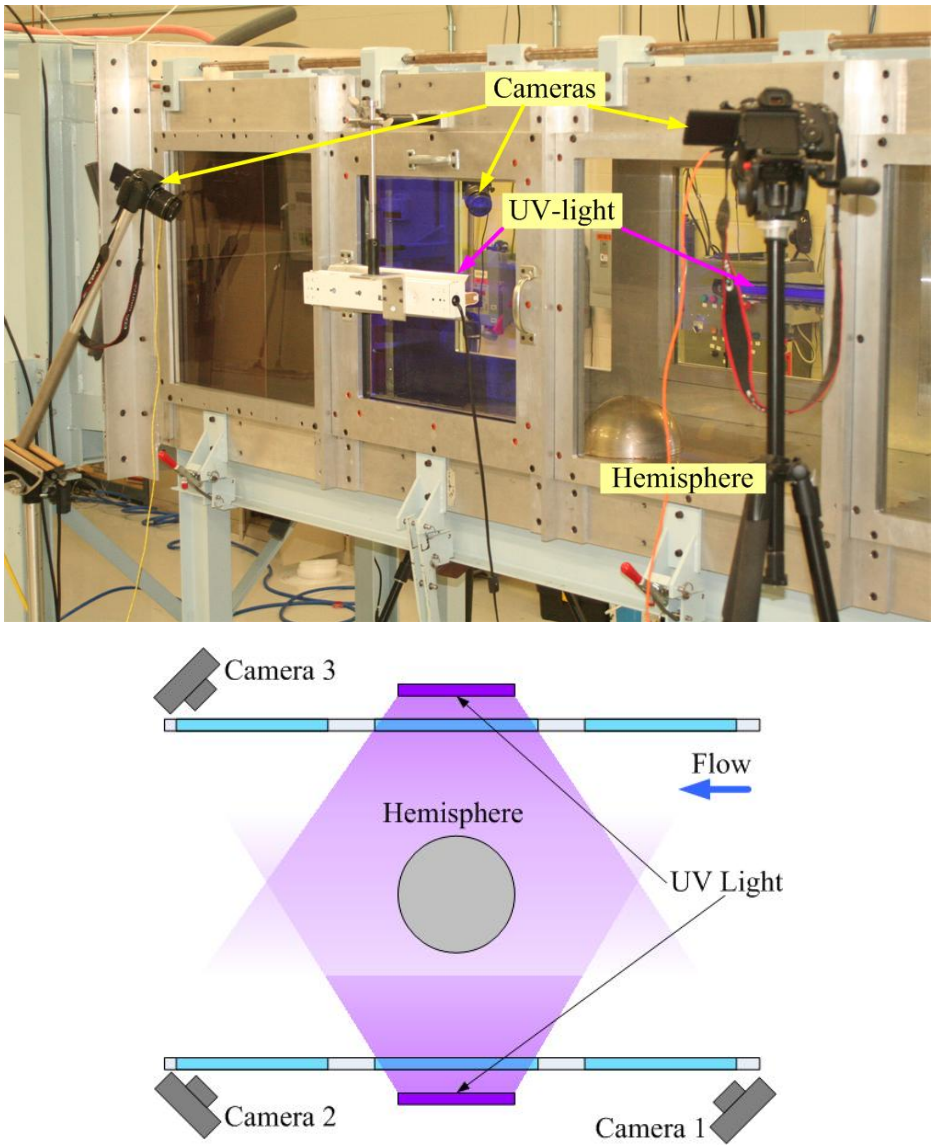

Figure 1. Set-up for surface oil visualization studies, picture (top) and the schematic (bottom).

To record temporal evolution of the local oil thickness, three Canon cameras were placed on both sides of the tunnel on tripods, see Figure 1. For each tested Mach number all cameras were trigged simultaneously every 5 seconds for 5-8 minutes total. Before each run, the oil was re-applied to assure approximately even oil distribution over the surface in the beginning of each run.

III. Data Processing

Collected images were used to reconstruct the temporal evolution of oil thickness over the full hemisphere surface and the adjacent tunnel wall using Perspective Transformation Matrix approach [11,12]. This approach allows to "project" oil-related intensities using simultaneous images from several different directions onto the "virtual" 3-D hemisphere and the adjacent wall. The perspective transformation allows to compute (X_I, Y_I)-location of the image point, if a 3-D coordinate of the object point, (X_O, Y_O, Z_O), shown in Figure 2, is given, as,

$$\begin{bmatrix} a \\ b \\ w \end{bmatrix} = PTM * \begin{bmatrix} X_O \\ Y_O \\ Z_O \\ 1 \end{bmatrix}, \quad X_I = a/w, \quad Y_I = b/w,$$

where *PTM* is the 3x4 Perspective Transformation Matrix, defined by the camera location and orientation angles. As accurate measurements of the camera orientation are difficult in practice, an alternative way to obtain a *PTM* is to take images of six or more non-coplanar points with known 3-D coordinates. After extracting 2-D locations of the points from the image, a *PTM* can be reconstructed using a least-square estimation [13]. The advantage of this method is that it does not require explicit knowledge of the camera's location and orientation. This approach was successfully implemented in reconstructing the unsteady pressure fields over hemisphere-on-cylinder turrets at subsonic speeds using pressure-sensitive paint technique [14].

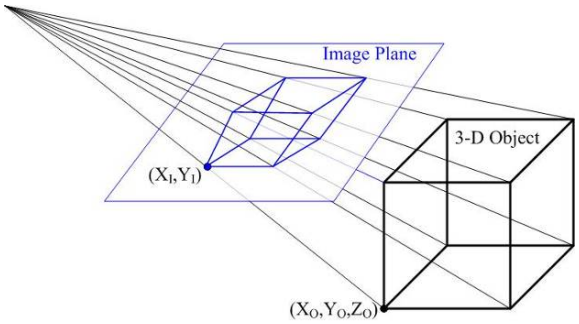

Figure 2. Schematic of perspective projection.

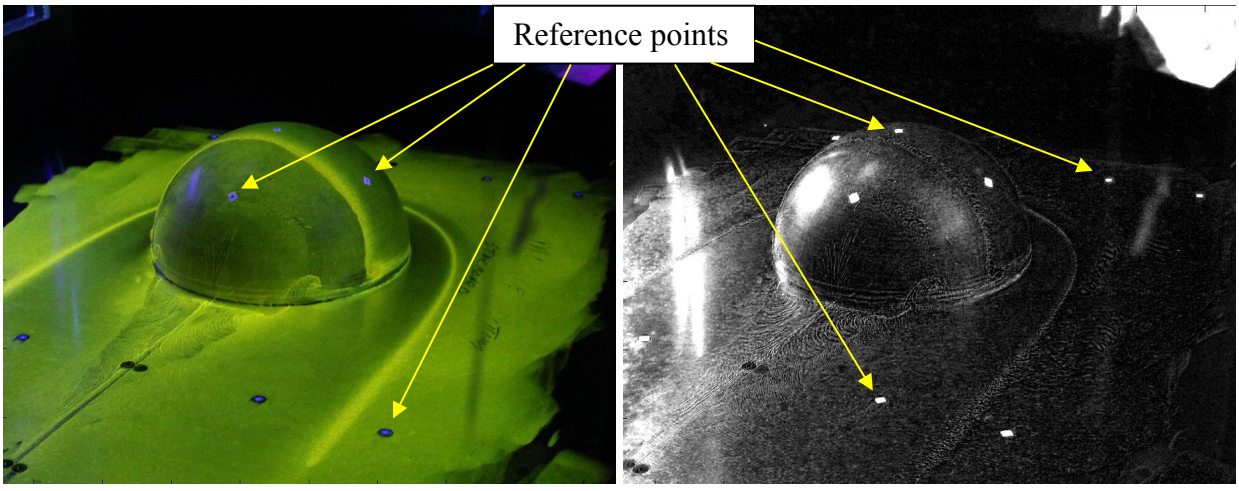

Figure 3. Hemisphere in the test section with several reference points marked by Scotch tape. Left: True color image. Right: Blue channel only.

Before the experiment, several reference points, 5 on the hemisphere and 8 at the tunnel wall, at known locations on the hemisphere and on the tunnel wall were marked by small square pieces of Scotch tape. A true color image of the test section with the reference points is shown in Figure 3, left; reference points appears to be in bluish color, as Scotch tape happened to glow blue under UV-light. Thus, to better locate reference points in every image, only blue channel from images was analyzed; Figure 3, right, shows the blue channel and all reference points are easily identifiable.

During each run, series of images were simultaneously taken by all three cameras. As the location of the reference points are known in 3-D space, after extracting 2-D locations of the points from images, a *PTM* was calculated for each camera. Although six non-co-planar points are sufficient to calculate a TMP matrix, 8 reference points for each camera were used to improve the accuracy of the TMP reconstruction.

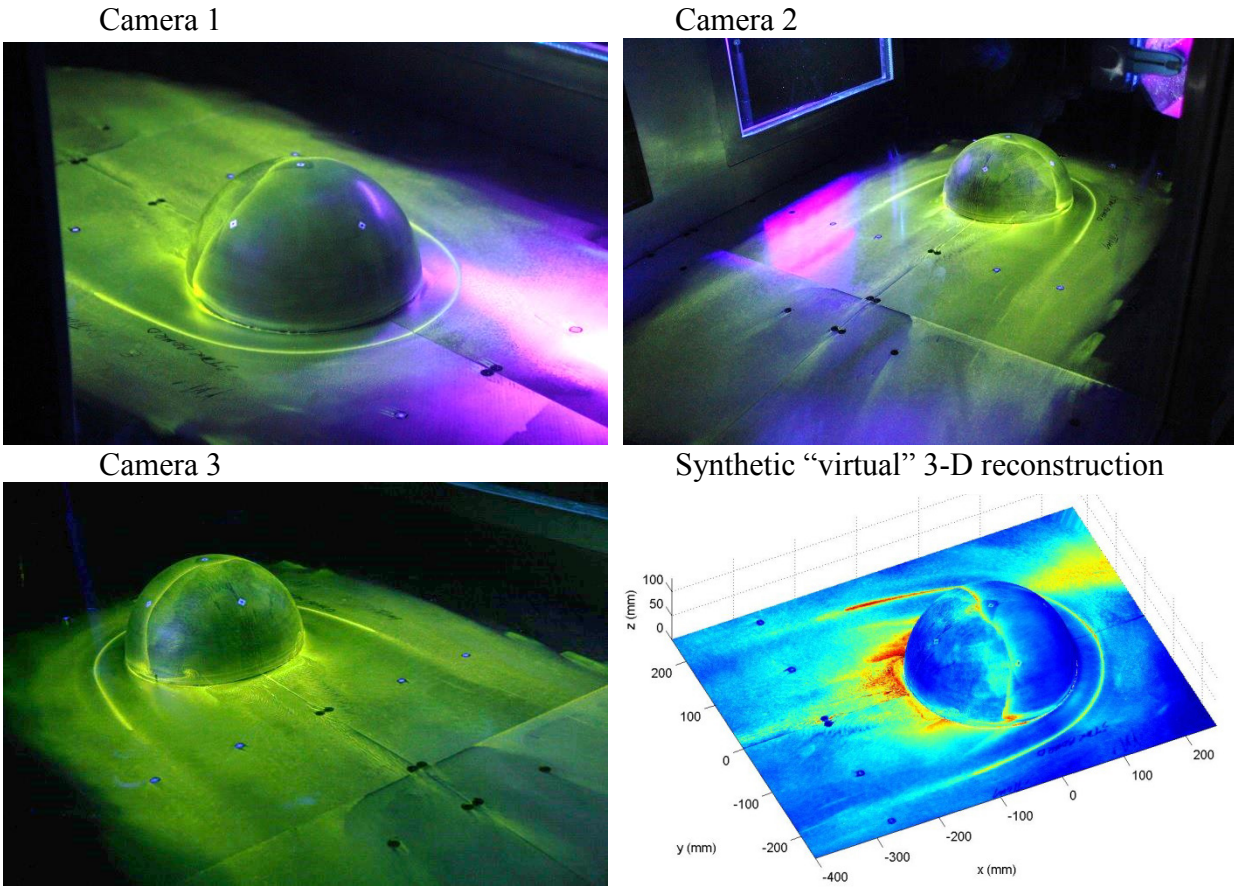

Figure 4. Simultaneous pictures of fluorescent oil on the surface of the hemisphere and the tunnel wall from all three cameras and the resulted "virtual" reconstructed oil luminescence in false color. Red color in the reconstructed image, bottom right, corresponds to regions with a thick oil layer and blue color corresponds to a thin oil layer.

The hemisphere and the tunnel wall surface were split into three regions to provide a unique mapping between the surface and the corresponding cameras' images and to "blend" data from different cameras. An example of a final 3-D reconstruction is shown in Figure 4, right

bottom, where individual images from Cameras 1, 2 and 3, also shown in Figure 4 were used to reconstruct oil luminescence on and around the "virtual" surface. To minimize the contaminating effect from UV-lights, seen as a bright purple spot in Cameras 1 and 2 in Figure 4, only the green channel was used in all images.

One important result of this projection is that the resulted "virtual" reconstruction can be viewed and studied from *any desired angle*, including the ones *not directly accessible* in the experiment.

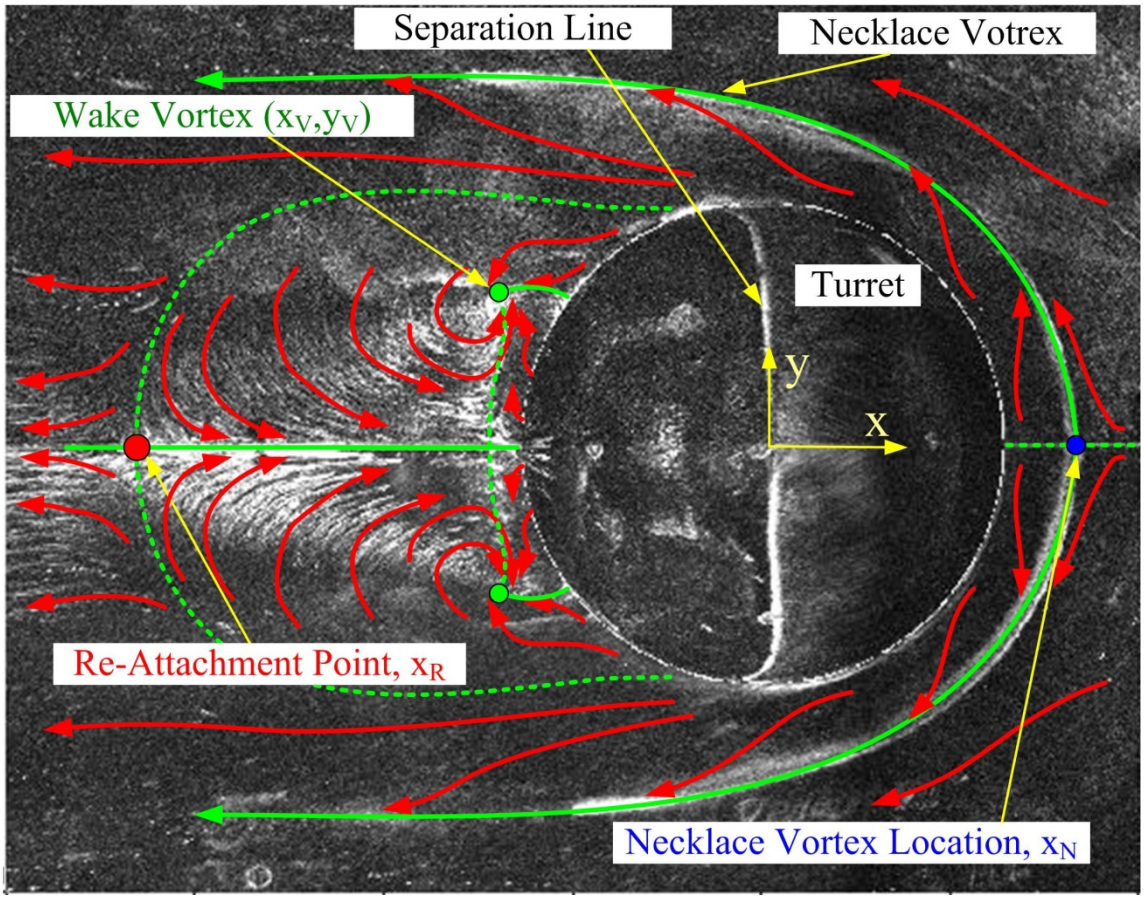

Figure 5. Topology of the surface streamlines around the hemisphere and definitions of topological features. Flow goes from right to left.

Finally, to better visualize surface streamlines, for each speed a mean intensity was removed from several consecutive frames and then all these frames were combined to have an enhanced image with longer oil streaks. These enhanced images will be presented in gray color in this paper, while instantaneous snapshots will be presented in false color, using colormap jet function in MATLAB.

IV. Results

To illustrate advantage of the "virtual" reconstruction and to better see the differences in the flow topology around the hemisphere at different transonic speeds, the top view of the oil luminescent intensity for M = 0.2 case is presented in Figure 5. The streamline pattern was

observed to be symmetric in the spanwise direction along the hemisphere centerplane for all Mach numbers tested. The origin of the system of coordinates was chosen to coincide with the hemisphere center, with the x-axis in the upstream direction and the y-axis in the cross-stream direction, all units are in millimeters. Several dominant topological features can be observed in Figure 5. A necklace vortex forms upstream of the hemisphere and extends downstream on both sides of the hemisphere. The flow is attached in the upstream half of the hemisphere and separates near the apex. The separated flow re-attaches downstream of the hemisphere. Also, an attached vortical structure, labelled a wake vortex in Figure 5, is formed in the separated region on the tunnel wall near the hemisphere on both sides. This surface topology around the hemisphere is similar to the one observed around a hemisphere-on-cylinder turrets [15,16,17].

Based on the streamline pattern, the flow topology was extracted and overlaid in the image in Figure 5; individual streamlines are shown in red and stable and unstable manifolds are shown as solid and dashed green line, respectively. Stable manifolds, like separation lines, attract streamlines and therefore can be easily seen in the image, as oil tends to collect along these stable manifolds; the separation line on the hemisphere and along the necklace vortex are two examples. Unstable manifolds, thus as re-attachment points or lines, tend to spread the oil out, so it is harder to identify them. One way to trace them is to look for regions of diverging streamlines, as around the re-attachment point, for example.

To investigate the evolution in topology at different Mach numbers, several topological features were extracted from the surface streamlines: the location of the re-attachment point, labeled as a red circle in Figure 5, the location of the wake vortex (green circle) and the most upstream location of the necklace vortex (blue circle). Top views of the enhanced images for each Mach number and presented in Figure 6, with the topological features marked. As the streamline pattern was observed to be symmetric in the spanwise direction along the hemisphere centerplane, only a half of the image is shown for each Mach number. Also, the locations of these topological features are summarized in Table 1.

Table 1. Locations of different topological features, defined in Figure 5, for all tested Mach numbers.

	x_R/D	x_V/D	y_V/D	x_N/D
M=0.2	-1.34	-0.55	0.31	0.64
M=0.5	-1.12	-0.56	0.22	0.67
M=0.6	-1.00	-0.50	0.26	0.67
M=0.7	-1.02	-0.47	0.32	0.67

At the lowest tested Mach number of 0.2, the separation region was fairly large, extending up to $x_R/D = -1.34$, where D is the hemisphere diameter. Also, the location of the wake vortex was relatively far away from the hemisphere. The location of the separation line on top of the hemisphere at 90 degrees had suggested that the boundary layer on top of the hemisphere was laminar or weakly turbulent; this observation is consistent with the large size of the separation region, as a laminar separation tends to re-attach further downstream, compared to a turbulent separation. This observed value of x_R/D also agrees with values between -1.2 and -1.5 observed for the low-Reynolds-number flows over hemispheres [18]. This result is somewhat surprising, as the Reynolds number for M = 0.2 is one million, which is well above the critical Reynolds number of 500,000, above which the separation on the hemisphere becomes laminar [2]. It would possibly require further investigation, as it was not the main objective of the current research.

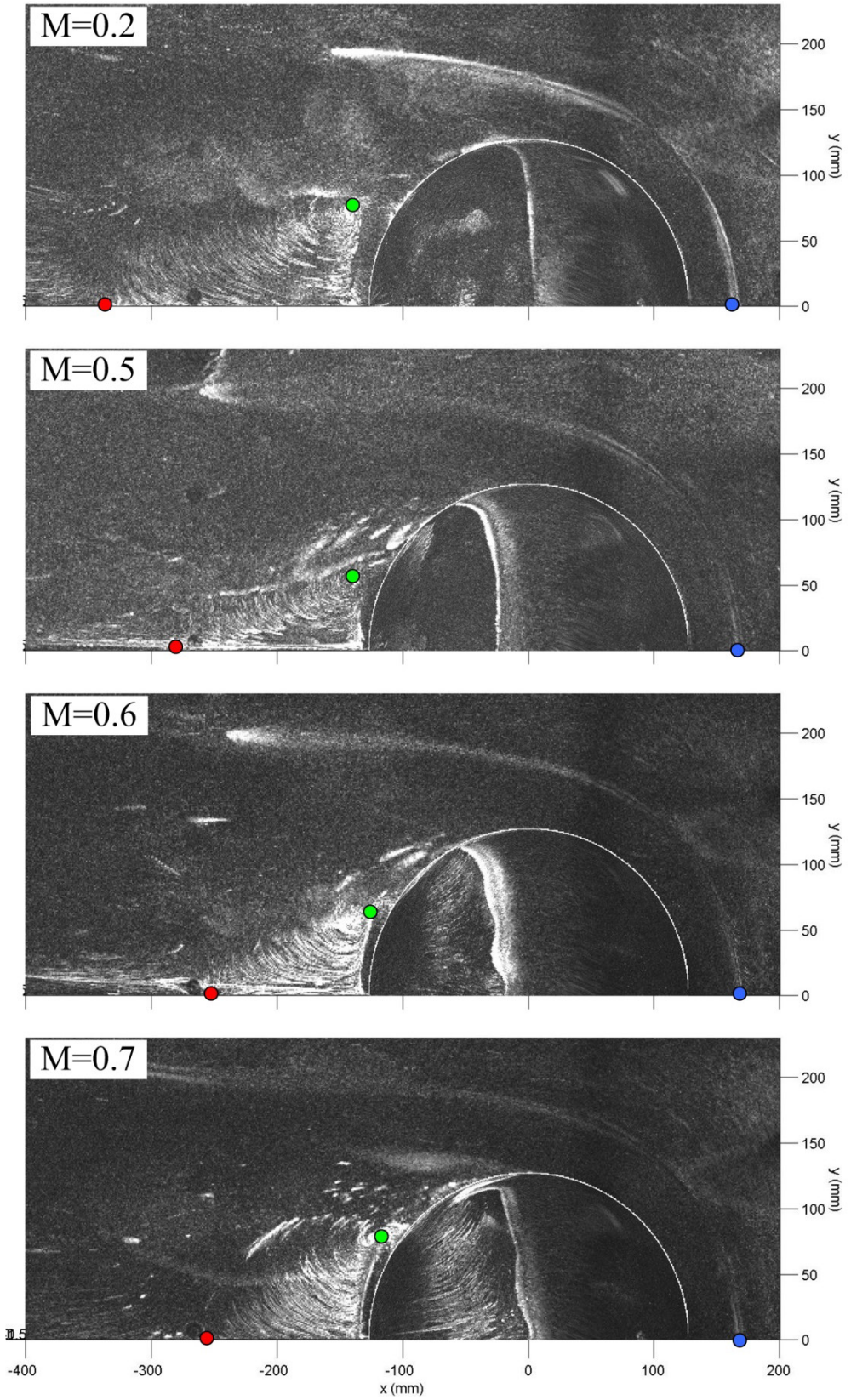

Figure 6. Top view of the reconstructed and enhanced oil luminescence (in gray color) over the hemisphere and the tunnel wall for all Mach numbers tested. Flow goes from right to left.

When the Mach number was increased to 0.5, the separation line on top of the hemisphere moved to approximately 100 degrees and the separation region shrank, with the separation point moving upstream to $x_R/D = -1.12$; all these factors indicate that the boundary layer became turbulent over the hemisphere. The wake vortex moved closer to the centerplane, from $y_V/D = 0.31$ for M = 0.2 to $y_V/D = 0.2$.

As mentioned in the Introduction, when the incoming Mach number is larger than 0.55, a local unsteady shock forms over the hemisphere [2]. However, at the incoming Mach number of 0.6 the shock is fairly weak [4,7] and does not significantly affect the separation line. Therefore the locations of the topological features for Mach numbers 0.5 and 0.6 are approximately the same, with the separation region slightly shrinking to an even smaller value of $x_R/D = -1$ and the wake vortex moving closer to the hemisphere. A similar value of $x_R/D = -1$for the re-attachment point was measured using series of unsteady pressure sensors downstream of the hemisphere [7]. Also, this value visually agrees with the analysis of the unsteady pressure field calculated around the hemisphere for the incoming Mach numbers of 0.8 [10].

At M = 0.7, the unsteady shock, formed on top of the hemisphere, became strong enough to force a premature separation on top of the hemisphere and causing the separation line on the hemisphere to move from 100 degrees back to 90 degrees; this is a well-known effect observed in both experiments [7,19] and numerical simulations [9,10]. The re-attachment point stay at the same location, as for M = 0.6 case and the wake vortex is been pushed away from the centerline, from $y_V/D = 0.26$ at M = 0.6 to $y_V/D = 0.32$. Also, as it will be shown later, the interaction of the unsteady shock with the separation line and the necklace vortex near the bottom of the hemisphere forces a formation of a large vortical structure, which might be responsible for shifting the wake vortex at this high Mach number.

As a last comment on the flow topology around the hemisphere, the location of the necklace vortex was observed to be largely unaffected by changes in the Mach number, except at the low Mach number of 0.2, where the necklace vortex was observed to be slightly closer to the hemisphere, see Table 1.

Examination of the changes in flow topology at the aft portion of the hemisphere, shown in Figure 7, revealed that the flow is symmetric relative to the centerplane and a dominant topological feature, a secondary vortex, indicated in Figure 7, is mostly unaffected by the Mach number.

The side views of the oil luminescence are shown in Figure 8. Red color corresponds to regions with a thick oil layer and blue color corresponds to a thin oil layer. Flow separation line over the hemisphere is clearly seen as narrow red lines, as oil moves toward separation lines and away from re-attachment lines. As discussed before, the separation line on the hemisphere clearly depends on Mach number. At M = 0.2, the flow separates around 90 degrees, indicating the laminar separation. For M = 0.5, the flow separates between 100 degrees (on top) and 110 degrees (near the bottom) on the aft portion of the hemisphere, consistent with static surface pressure measurements [2]. Also, a small vortical structure is visible near the bottom of the hemisphere in Figure 8. At M = 0.6, a weak shock forms near the top of the hemisphere, but it is not strong enough to change the separation line and other topological features on the turret, see Figure 8. However, at a higher Mach number of 0.7, the shock on top of the hemisphere grows stronger, forcing a premature flow separation around 90 degrees. The side vortical structure, marked in Figure 8, bottom plot, grows larger and moves away from the wall, while the secondary vortex somewhat weakens at this speed, see bottom plot in Figure 7. A similar large

vortical structure formation was observed in numerical simulations of the flow around a hemisphere for M = 0.85 [9].

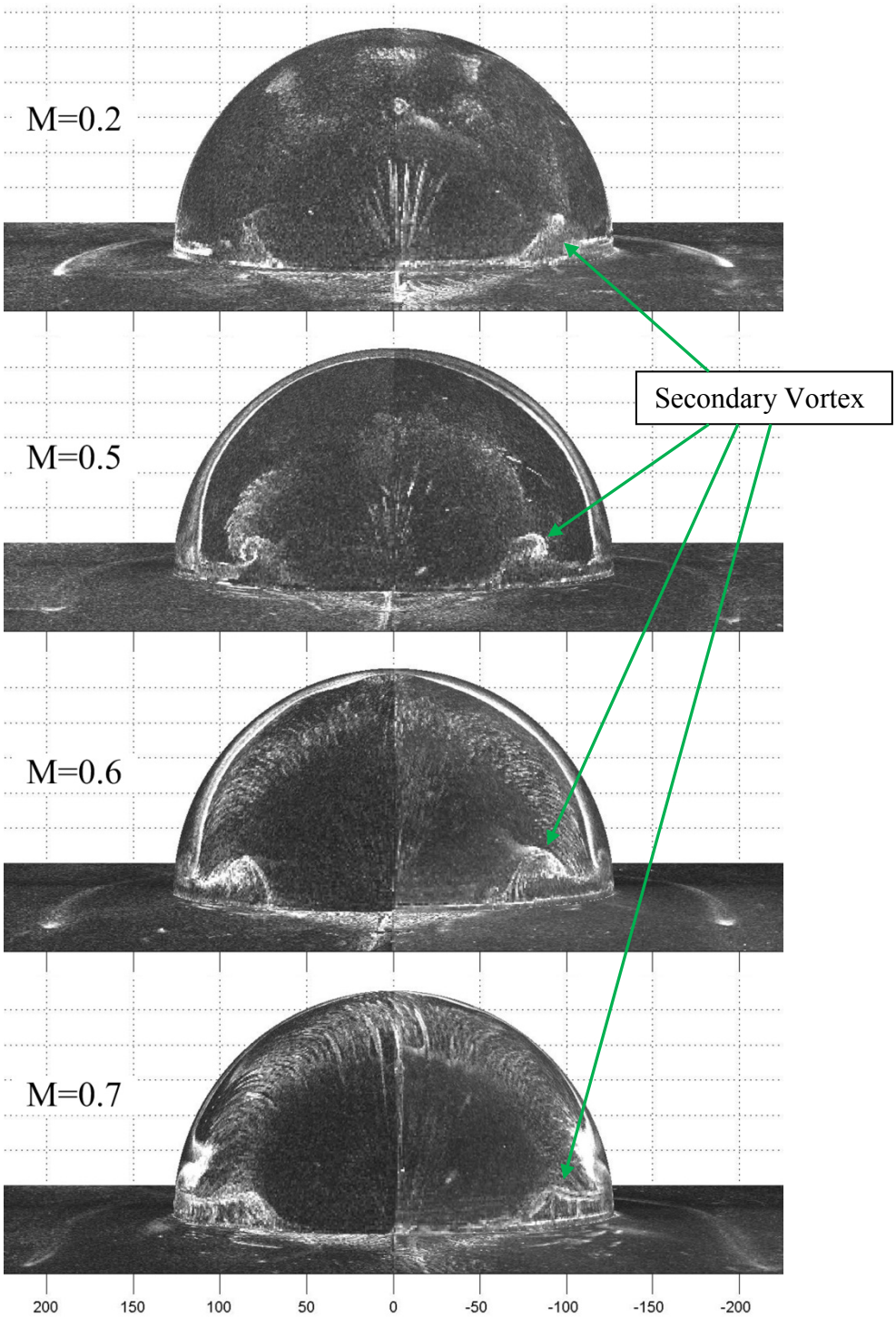

Figure 7. Back view of the reconstructed and enhanced oil luminescence (in gray color) over the hemisphere and the tunnel wall for all Mach numbers tested. Flow goes outward of the page.

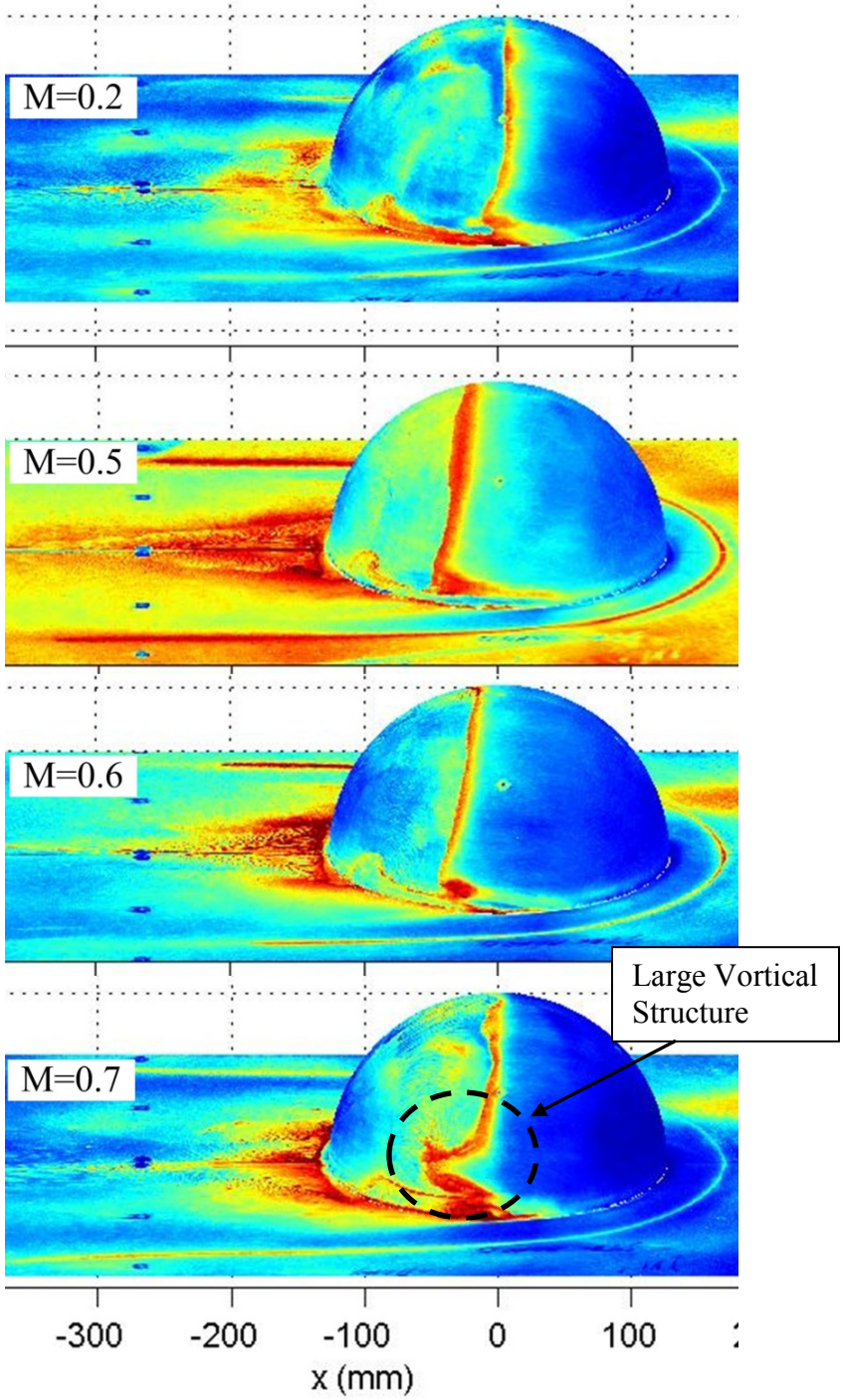

Figure 8. Side view of the reconstructed oil thickness (in false color) over the hemisphere and the tunnel wall for all measured Mach numbers. Flow goes from right to left.

Knowing the details of the topology of the flow around the turret, the variation in the separation region with Mach number can be qualitatively explained as follows. When the separation is laminar, it occurs on top of the hemisphere, where the local velocity is parallel to the wall, as schematically shown in Figure 9, top. Downwash force from the necklace vortex will eventually push the flow toward the wall, forming a finite, bur fairly large separation region, see

Figure 6, top. When the separation is turbulent, it occurs on the downstream portion of the hemisphere, so the local velocity has a downward component, see Figure 9, middle; this will result in a smaller separation region, as it was observed for M = 0.5 and 0.6 in Figure 6. When the shock forms on top of the hemisphere, the separation moves upstream to the top of the hemisphere, so the separation region should have been increased. But the formation of the large vortical structure, which has the same circulation sign as the necklace vortex is believed to interact and eventually to increase the strength of the necklace vortex downstream of the turret. This effect will result in increased downwash force, see Figure 9, bottom, forcing the separation region to be smaller. These opposite trends would cancel each other, so the separation region will stay approximately the same, as it was observed for M = 0.7 in Figure 6. At even larger transonic and low supersonic speeds the shock-induced separation moves downstream on the hemisphere, adding a downward component to the local velocity, so the separation region will continue to decrease in size at these speeds, as it was observed in numerical simulations [10].

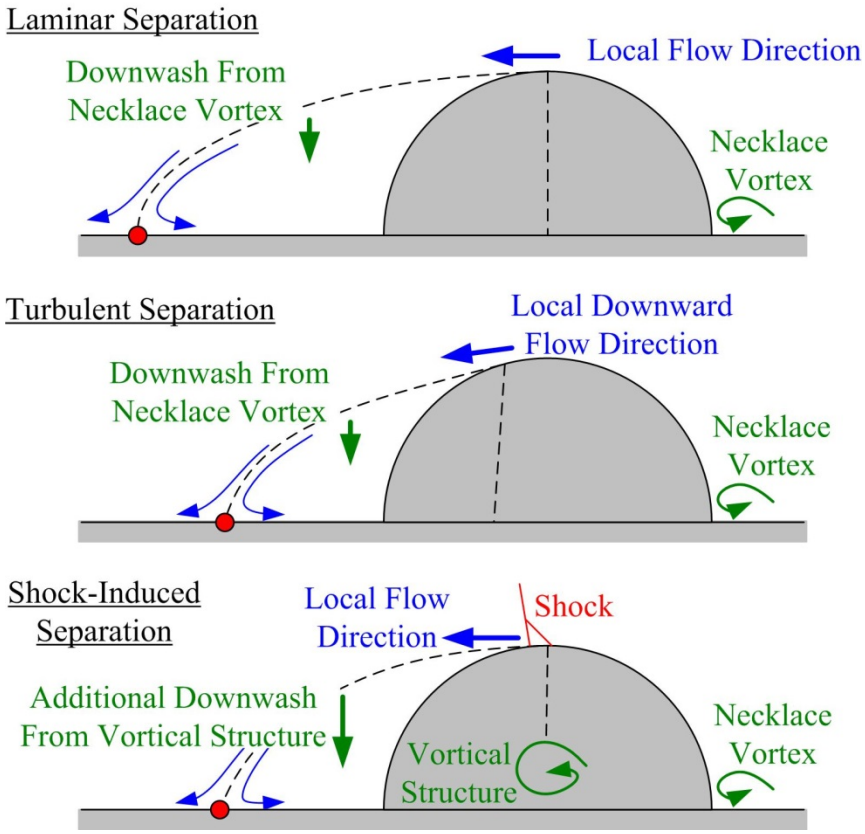

Figure 9. Schematic of the flow topology when the separation on top of the hemisphere is laminar (top), turbulent (middle) and shock-induced (bottom). Flow goes from right to left. In the bottom plot, the presence of the large vortical structure is believed to be responsible for additional downwash in the transonic regime.

As the vortical structure at high transonic speeds creates both the steady pressure drop in the center of it, as well as increased unsteady pressure fluctuations due to increased interaction with the separated line and the necklace vortex, it will undoubtedly adversely affect the aero-optical performance of the hemispherical turret at low side-viewing angles, when the outgoing beam will traverse through this unsteady vortical structure.

Finally, a word of caution should be given when using oil for flow visualization in some sensitive regions or regimes of the flow. As oil accumulates near the separation lines, it will create a fluidic-type roughness on a surface and potentially modify the flow of interest. An example of such interference was observed in this experiment at M = 0.6. For relatively short tunnel running times the streamline pattern was spanwise symmetric with respect to the centerline, is shown in Figure 10, left. But for longer running times of approximately 6 minutes or longer, oil significantly accumulated near the separation line on the hemisphere, but, as the distribution was not spanwise-symmetric, it resulted in asymmetric tripping of the flow, which in turn resulted in the spanwise-distorted separation region and eventually made the streamline pattern spanwise asymmetric, see an example of the surface flow after a longer tunnel run in Figure 10, right.

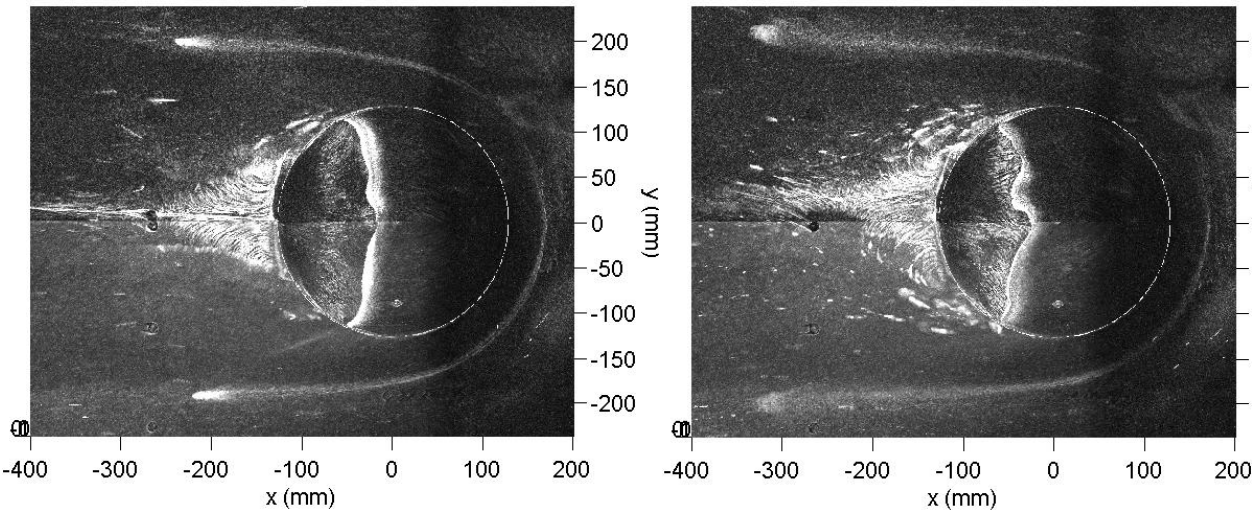

Figure 10. Top view of the reconstructed and enhanced oil luminescence (in gray color) over the hemisphere and the tunnel wall after 3 minutes (left) and 8 minutes (right) of the tunnel running. Incoming Mach number is 0.6.

V. Conclusions

Time-resolved measurements of surface flow topology on and around the hemisphere using fluorescent oil were conducted in the tunnel in a range of subsonic and transonic speeds, using several cameras. The cameras were synchronized and simultaneous images of the oil evolution on the hemisphere surface and adjacent tunnel wall were collected from different viewing angles over the course of several minutes of the tunnel running time. These images were used to reconstruct oil luminescence pattern over the "virtual" surface of the interest. It allows studying oil patterns from any desired angles, not limited to the ones, used in the experiment.

Inspection of the surface streamlines revealed that the surface flow is symmetrical in the spanwise direction for all Mach numbers tested. The separation region was found to be the largest at the smallest tested Mach number of 0.2 and progressively shrinking in size when the increasing Mach number. The separation line on the hemisphere was around 90 degrees for the smallest Mach number, extending to 100-110 degrees for M = 0.5 and 0.6 and retreating back to 90 degrees at M = 0.7 due to the presence of the unsteady shock, formed over the hemisphere at this transonic speed. Also, a formation of a large vortical structure on both sides of the hemisphere near the tunnel wall was observed at this Mach number. It is expected that this

vortical structure will impose additional aero-optical distortions for an airborne side-mounted hemispherical turret at high transonic speeds for low side-looking angles.

Acknowledgements

This work was funded by the Air Force Research Laboratory, Directed Energy Directorate. The U.S. Government is authorized to reproduce and distribute reprints for governmental purposes notwithstanding any copyright notation thereon.

References

[1] M. Wang, A. Mani and S. Gordeyev, "Physics and Computation of Aero-Optics", *Annual Review of Fluid Mechanics*, Vol. **44**, pp. 299-321, 2012.

[2] S. Gordeyev and E. Jumper, "Fluid Dynamics and Aero-Optics of Turrets", *Progress in Aerospace Sciences*, **46**, (2010), pp. 388-400.

[3] Fang S, Disotell KJ, Long SR, Gregory JW, Semmelmayer FC, Guyton RW "Application of Fast-Responding Pressure-Sensitive Paint to a Hemispherical Dome in Unsteady Transonic Flow", *Experiments in Fluids*, **50**(*6*), pp.1495-1505, 2011.

[4] J. Morrida, S. Gordeyev, N. De Lucca, E. Jumper, "Aero-Optical Investigation of Transonic Flow Features and Shock Dynamics on Hemisphere-On-Cylinder Turrets", AIAA Paper 2015-0676, 2015.

[5] E.J. Jumper, S. Gordeyev, D. Cavalieri, P. Rollins, M.R. Whiteley and M.J. Krizo, "Airborne Aero-Optics Laboratory - Transonic (AAOL-T)",AIAA Paper 2015-0675, 2015.

[6] B. Vukasinovic, A. Glezer, S. Gordeyev, E. Jumper and V. Kibens, "Active Control and Optical Diagnostics of the Flow over a Hemispherical Turret", AIAA Paper 2008-0598, 2008.

[7] J. Morrida, S. Gordeyev, E. Jumper, S.Gogineni, and D.J. Wittich, "Investigation of Shock Dynamics on a Hemisphere Using Pressure and Optical Measurements", to be presented at 54th AIAA Aerospace Sciences Meeting, San Diego, California, 4 - 8 January 2016.

[8] A. Vorobiev, S. Gordeyev, E. Jumper, S.Gogineni, A. Marruffo and D.J. Wittich, "Low-Dimensional Dynamics and Modeling of Shock-Separation Interaction over Turrets at Transonic Speeds", AIAA Paper 2014-2357, 2014.

[9] Jelic R, Sherer S, Greendyke R, "Simulation of Various Turrets at Subsonic and Transonic Flight Conditions Using OVERFLOW" *Journal of Aircraft*, **50**, pp.398-409, 2013.

[10] Coirier, W.J., Porter, C., Barker, J., Stutts, J., Whiteley, M., Goorsky, D. and Drye, R. "Aero-Optical Evaluation of Notional Turrets in Subsonic, Transonic and Supersonic Regimes", AIAA Paper 2014-2355, 2014.

[11] Carlbom I, Paciorek J, "Planar Geometric Projections and Viewing Transformations", *ACM Computing Surveys*, **10**(*4*), pp. 465–502, 1978.

[12] Haralick RM, "Using Perspective Transformations in Scene Analysis", *Computer Graphics and Image Processing*, **13**, pp. 191-221, 1980.

[13] Tan TN, Sullivan GD, Baker KD, "On computing the perspective transformation matrix and camera parameters", In*: Proc. of 4th British Machine Vision Conf., Surrey, England*, pp. 125–134, 1993.

[14] S. Gordeyev, N. De Lucca, E. Jumper, K. Hird, T.J. Juliano, J.W. Gregory, J. Thordahl and D.J. Wittich, " Comparison of Unsteady Pressure Fields on Turrets with Different Surface Features using Pressure Sensitive Paint ", *Experiments in Fluids*, **55**, p. 1661, 2014.

[15] Gordeyev, S., Post, M., McLaughlin, T., Ceniceros, J., and Jumper, E.,"Aero-Optical Environment Around a Conformal-Window Turret," *AIAA Journal*, **45**(*7*), pp. 1514–1524, 2007.
[16] B. Vukasinovic, A. Glezer, S.Gordeyev, E. Jumper and V. Kibens, "Hybrid Control of a Turret Wake", *AIAA Journal*, **49**(*6*), pp. 1240-1255, 2011.
[17] P. E. Morgan and M. R. Visbal, "Hybrid Reynolds-Averaged Navier–Stokes/Large-Eddy Simulation Investigating Control of Flow over a Turret", *Journal of Aircraft*, **49**(*6*), pp. 1700--1717, 2012.
[18] M.M. Tavakol, M. Yaghoubi and M. Masoudi Motlagh, "Air flow aerodynamic on a wall-mounted hemisphere for various turbulent boundary layers", *Experimental Thermal and Fluid Science*, **34**, pp. 538–553, 2010.
[19] Fang S, Disotell KJ, Long SR, Gregory JW, Semmelmayer FC and Guyton RW, "Application of fast-responding pressure-sensitive paint to a hemispherical dome in unsteady transonic flow", *Experiments in Fluids*, **50**(*6*), pp.1495–1505, 2011.